

- ments of CaM in the ternary Ca^{2+} -CaM-M13 complex were obtained in 3D double and triple resonance NMR experiments [M. Ikura, L. E. Kay, A. Bax, *Biochemistry* **29**, 4569 (1990); A. Bax, G. M. Clore, A. M. Gronenborn, *J. Magn. Reson.* **88**, 425 (1990); G. M. Clore, A. Bax, P. C. Driscoll, P. T. Wingfield, A. M. Gronenborn, *Biochemistry* **29**, 8172 (1990); G. M. Clore and A. M. Gronenborn, *Prog. Nucl. Magn. Reson.* **23**, 43 (1991)].
18. G. Wider, C. Weber, R. Traber, H. Widmer, K. Wüthrich, *J. Am. Chem. Soc.* **112**, 9015 (1990).
19. M. Ikura, L. E. Kay, R. Tschudin, A. Bax, *J. Magn. Reson.* **86**, 204 (1990); E. R. P. Zuiderweg, L. P. McIntosh, F. W. Dahlquist, S. W. Fesik, *ibid.*, p. 210.
20. S. W. Fesik and E. R. P. Zuiderweg, *ibid.* **78**, 588 (1988); D. Marion, L. E. Kay, S. W. Sparks, D. A. Torchia, A. Bax, *J. Am. Chem. Soc.* **111**, 1515 (1989); D. Marion *et al.*, *Biochemistry* **29**, 6150 (1989).
21. G. M. Clore, L. E. Kay, A. Bax, A. M. Gronenborn, *Biochemistry* **30**, 12 (1991).
22. E. R. P. Zuiderweg, A. M. Petros, S. W. Fesik, E. T. Olejniczak, *J. Am. Chem. Soc.* **113**, 370 (1991).
23. G. M. Clore *et al.*, *EMBO J.* **5**, 2729 (1986).
24. Upper distance limits for distances involving methyl and methylene protons were corrected appropriately for center averaging [K. Wüthrich, M. Billeter, W. Braun, *J. Mol. Biol.* **169**, 949 (1983)]. In addition, 0.5 Å was added to the upper limit of distances involving methyl protons to account for the higher apparent intensity of methyl resonances [G. M. Clore, A. M. Gronenborn, M. Nilges, C. A. Ryan, *Biochemistry* **26**, 8012 (1987)].
25. K. Wüthrich, *NMR of Proteins and Nucleic Acids* (Wiley, New York, 1986).
26. A. Pardi, M. Billeter, K. Wüthrich, *J. Mol. Biol.* **180**, 741 (1984).
27. The coordinates of the 24 SA structures and of the restrained minimized mean structure, (SA)_r, together with the experimental restraints, have been deposited in the Brookhaven Protein Data Bank.
28. M. Nilges, G. M. Clore, A. M. Gronenborn, *FEBS Lett.* **229**, 317 (1988).
29. The hybrid distance geometry-simulated annealing protocol for (27) makes use of the program XPLOR [A. T. Brünger, G. M. Clore, A. M. Gronenborn, M. Karplus, *Proc. Natl. Acad. Sci. U.S.A.* **83**, 3801 (1986); A. T. Brünger, *XPLOR Version 3 Manual* (Yale University, New Haven, 1992)] incorporating a distance geometry module (J. Kuszewski, M. Nilges, A. T. Brünger, *J. Biomol. NMR* **2**, 33 (1992)). The protocol involves first calculating an initial set of substructures incorporating only about one-third of the atoms by projection from *n*-dimensional distance space into cartesian coordinate space, followed by simulated annealing with all atoms. The target function that is minimized during simulated annealing (as well as in conventional Powell minimization) comprises only quadratic harmonic potential terms for covalent geometry (that is, bonds, angles, planes, and chirality), square-well quadratic potentials for the experimental distance and torsion angle restraints (22), and a quartic van der Waals repulsion term for the nonbonded contacts (26). All peptide bonds were restrained to be trans. There are no hydrogen bonding, electrostatic, or 6-12 Lennard-Jones potential terms in the target function.
30. The coordinates used have the Brookhaven Protein Data Bank accession number 3CLN [Y. S. Babu, C. E. Bugg, W. J. Cook, *J. Mol. Biol.* **204**, 191 (1988)].
31. D. Eisenberg and A. D. McLaglan, *Nature* **319**, 199 (1986); L. Cliche, L. M. Gregoret, F. E. Cohen, P. A. Kollman, *Proc. Natl. Acad. Sci. U.S.A.* **87**, 3240 (1990).
32. The changes in accessible surface area and solvation free energy calculated for M13 peptide are relative to that of the free peptide in the same helical conformation. Relative to a theoretical extended, unfolded structure, the decrease in accessible surface area and solvation free energy of M13 upon binding is 2039 Å² and 29 kcal mol⁻¹, respectively.
33. S. Spera, M. Ikura, A. Bax, *J. Biomol. NMR* **1**, 155 (1991).
34. A. Persechini *et al.*, *J. Biol. Chem.* **264**, 8052 (1989); M. Kataoka, J. F. Head, A. Persechini, R. H. Kretsinger, D. M. Engelmann, *Biochemistry* **30**, 1188 (1991).
35. K. T. O'Neil, S. Erickson-Viitanen, W. F. DeGrado, *J. Biol. Chem.* **264**, 14571 (1989).
36. T. J. Lukas, W. H. Burgess, F. G. Prendergast, W. Lau, D. M. Watterson, *Biochemistry* **25**, 1458 (1986).
37. D. K. Blumenthal and E. G. Krebs, *Methods Enzymol.* **139**, 115 (1987).
38. M. Kataoka, J. F. Head, T. Vorherr, J. Krebs, E. Carafoli, *Biochemistry* **30**, 6247 (1991).
39. M. J. Hubbad and C. B. Klee, *ibid.* **28**, 1867 (1989); D. Guerini and C. B. Klee, *Adv. Protein Phosphatases* **6**, 391 (1991).
39. B. Kemp, R. Pearson, V. Guerriero, I. Bagchi, A. Means, *J. Biol. Chem.* **262**, 2542 (1987).
40. M. Dasgupta, T. Honeycutt, D. K. Blumenthal, *ibid.* **264**, 17156 (1989).
41. J. Trehwella, D. K. Blumenthal, S. E. Rokop, P. A. Seeger, *Biochemistry* **29**, 9316 (1990).
42. H. Charbonneau *et al.*, *ibid.* **30**, 7931 (1991); J. P. Novack, H. Charbonneau, J. K. Bentley, K. A. Walsh, J. A. Beavo, *ibid.*, p. 7940.
43. M. K. Bennett and M. B. Kennedy, *Proc. Natl. Acad. Sci. U.S.A.* **84**, 1794 (1987); R. M. Hanley *et al.*, *Science* **237**, 293 (1987).
44. A. P. Kwiatkowski and M. M. King, *Biochemistry* **28**, 5380 (1989).
45. L. E. Kay, D. Marion, A. Bax, *J. Magn. Reson.* **84**, 72 (1989).
46. G. Zhu and A. Bax, *ibid.* **90**, 405 (1990).
47. D. S. Garrett, R. Powers, A. M. Gronenborn, G. M. Clore, *ibid.* **95**, 214 (1991).
48. B. R. Brooks *et al.*, *Comput. Chem.* **4**, 187 (1983).
49. M. Carlson, *J. Mol. Graphics* **5**, 103 (1987).
50. D. K. Blumenthal *et al.*, *Proc. Natl. Acad. Sci. U.S.A.* **82**, 3187 (1985).
51. R. B. Pearson *et al.*, *Science* **241**, 970 (1988); C. J. Foster, *Arch. Biochem. Biophys.* **280**, 397 (1990).
52. A. K. Verma *et al.*, *J. Biol. Chem.* **263**, 14152 (1988).
53. T. Ono, G. T. Slaughter, R. G. Cook, A. T. Means, *ibid.* **264**, 2081 (1989).
54. R. L. Kincaid, M. S. Nightingale, B. R. Martin, *Proc. Natl. Acad. Sci. U.S.A.* **85**, 8983 (1988); C. B. Klee, unpublished data.
55. D. A. Malencik and S. R. Anderson, *Biochem. Biophys. Res. Commun.* **114**, 50 (1983).
56. Supported by the AIDS Targeted Anti-Viral Program of the Office of the Director of the National Institutes of Health (G.M.C., A.M.G., and A.B.). We thank K. Bechingham and J. Maune for providing us with the *Drosophila* calmodulin coding construct.

31 January 1992; accepted 27 March 1992

Modulation of an NCAM-Related Adhesion Molecule with Long-Term Synaptic Plasticity in *Aplysia*

Mark Mayford, Ari Barzilai, Flavio Keller,*
Samuel Schacher, Eric R. Kandel

A form of learning in the marine mollusk *Aplysia*, long-term sensitization of the gill- and siphon-withdrawal reflex, results in the formation of new synaptic connections between the presynaptic siphon sensory neurons and their target cells. These structural changes can be mimicked, when the cells are maintained in culture, by application of serotonin, an endogenous facilitating neurotransmitter in *Aplysia*. A group of cell surface proteins, designated *Aplysia* cell adhesion molecules (apCAM's) was down-regulated in the sensory neurons in response to serotonin. The deduced amino acid sequence obtained from complementary DNA clones indicated that the apCAM's are a family of proteins that seem to arise from a single gene. The apCAM's are members of the immunoglobulin class of cell adhesion molecules and resemble two neural cell adhesion molecules, NCAM and fasciclin II. In addition to regulating newly synthesized apCAM, serotonin also altered the amount of preexisting apCAM on the cell surface of the presynaptic sensory neurons. By contrast, the apCAM on the surface of the postsynaptic motor neuron was not modulated by serotonin. This rapid, transmitter-mediated down-regulation of a cell adhesion molecule in the sensory neurons may be one of the early molecular changes in long-term synaptic facilitation.

One mechanism for storing long-term memory in neurons is by the formation of new synaptic connections. For example, studies of the gill- and siphon-withdrawal reflex of the mollusk *Aplysia californica* show that, after long-term sensitization, there is an increase in the number of synaptic connections made by identified siphon sensory neurons on their target cells, such as the gill motor neuron L7 (1). These changes last several weeks and parallel the behavioral changes produced by the training. Similar-

ly, stimuli that produce long-term potentiation (LTP) in the hippocampus of vertebrates produce changes in the structure and distribution of synapses between the pre- and postsynaptic cells (2).

In *Aplysia*, these structural changes can be studied in identified neurons maintained in dissociated cell culture (3, 4). Individual sensory and motor neurons form functional synaptic connections in culture that undergo long-term synaptic facilitation in response to repeated applications of serotonin (5-HT), an

endogenous facilitating neurotransmitter in *Aplysia* (5, 6). In addition, 5-HT produces structural changes in the presynaptic sensory neuron in vitro that are similar to those produced in the intact animal by sensitization training (7). Thus, the formation of new synaptic connections may contribute to the maintenance of long-term facilitation.

Paralleling the results of behavioral experiments, inhibitors of either protein or RNA synthesis block long-term, but not short-term, facilitation when applied during, or shortly after, exposure to 5-HT (5). To study the molecular changes that underlie long-term facilitation, Barzilai and co-workers used quantitative two-dimensional gel electrophoresis and found that 5-HT produced an increase in [³⁵S]methionine incorporation into ten protein spots (E₁ to E₁₀) and a decrease in labeling of five spots (D₁ to D₅) (8). The change in these proteins was rapid and transient, with peak increases or decreases occurring within 15 to 60 minutes and returning to baseline values by 3 hours. The changes in labeling of these proteins may reflect either an alteration in the amount of their mRNA, the rate of its translation, or a change in the half-life of the protein itself.

We have now characterized four of the five proteins that decrease in labeling in response to 5-HT. This group of proteins, D₁ to D₄ (8), ranges in molecular size from 100 to 140 kilodaltons (kD) (Fig. 1, A and B). Analogs of adenosine 3',5'-monophosphate (cyclic AMP), which is activated by 5-HT and can produce long-term facilitation and the accompanying structural changes (9), also down-regulate D₁ to D₄ in the sensory neurons (Fig. 1C and Table 1). Moreover, the down-regulation of D₁ to D₄ produced by 5-HT can be enhanced by the addition of 3-isobutyl-1-methylxanthine (IBMX), an inhibitor of cyclic AMP phosphodiesterase. As is the case with the long-term structural and functional changes, the down-regulation induced by 5-HT and by cyclic AMP is blocked by actinomycin D, an inhibitor of RNA synthesis (Fig. 1B and Table 1). The four proteins are related; they show similar peptide maps and each protein cross-reacts with two monoclonal antibodies (MAB's), 4E8 and 3D9, produced against membranes from the *Aplysia* central nervous system (CNS) (10). The four proteins that are immunoprecipitated

by MAB 4E8 comigrate on two-dimensional gels with proteins D₁ to D₄ (Fig. 1A). The MAB's define a group of *Aplysia* glycoproteins that are specific to the nervous system and found on the surface of neurites and growth cones of cultured neurons (10).

Cloning and characterization of apCAM. To characterize these proteins structurally, we used the MAB's to obtain cDNA clones coding for proteins in the D₁ to D₄ group. An *Aplysia* CNS cDNA library constructed in the expression vector λgt11 was screened with MAB 4E8. One immunoreactive plaque was obtained and used to probe a randomly primed cDNA library. Three independent clones (d12, d15, and d19) were obtained that contained open reading frames capable of coding for proteins of 84, 88, and

102 kD, respectively (Fig. 2A). Each open reading frame coded for two sequences, which were identical to amino acid sequences obtained from protein spot D₁ and from protein isolated with the use of MAB 4E8. This confirms that the cDNA's code for proteins in the D₁ to D₄ group and that MAB 4E8 reacts with this group of proteins.

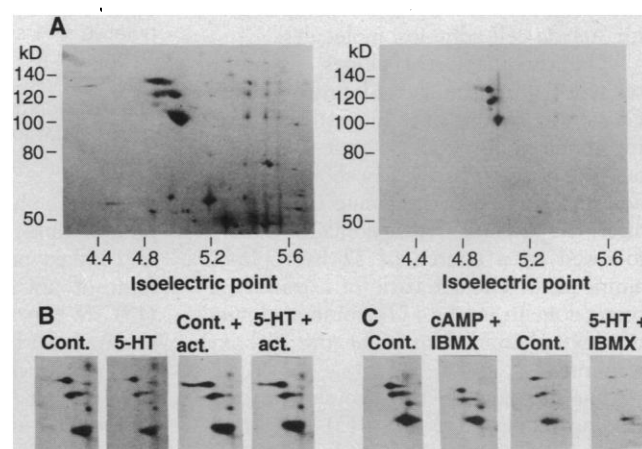
An analysis of the clones indicates that they encode three related proteins that can be divided into shared as well as distinctive domains (Fig. 2B). In all three predicted proteins, the 734 amino acids at the amino terminus are identical; and the proteins begin with a typical hydrophobic signal peptide sequence that predicts a glutamine amino terminus for the mature proteins (11). The signal peptide sequence is fol-

Table 1. Down-regulation of apCAM expression by 5-HT and 8-(4-chlorophenylthio) (CFT)—cyclic AMP. *Aplysia californica* pleural sensory clusters were dissected and labeled with [³⁵S]methionine for 30 minutes (except for 20 μM 5-HT plus 100 μM IBMX, which was labeled for 60 minutes), and proteins were resolved by two-dimensional gel electrophoresis as in Fig. 1. Data are expressed as the ratio of the amount of the protein (D₁, D₂, D₃, or D₄) in the test situation to the amount in control conditions (mean ± SEM), calculated as in (8).

Condition	Time (minutes)	D ₁	D ₂	D ₃	D ₄	n
5-HT (5 μM)	30	0.75 ± 0.08**	0.67 ± 0.1*	0.68 ± 0.09***	0.70 ± 0.11*	8
5-HT (5 μM), actinomycin D (100 μg/ml)	30	1.07 ± 0.07†	1.44 ± 0.50†	0.94 ± 0.06†	1.07 ± 0.07†	4
5-HT (20 μM), IBMX (100 μM)	60	0.63 ± 0.12*	0.37 ± 0.22*	0.37 ± 0.11***	0.32 ± 0.10***	5
CFT-cAMP (100 μM), IBMX (100 μM)	120	0.66 ± 0.11*	0.10 ± 0.11***	0.62 ± 0.12*	0.69 ± 0.10*	4
CFT-cAMP (100 μM), IBMX (100 μM), actinomycin D (100 μg/ml)	120	1.17 ± 0.14†	0.93 ± 0.30†	1.05 ± 0.16†	1.10 ± 0.26†	4

*P < 0.05; **P < 0.02; ***P < 0.01. † Not significant.

Fig. 1. Effect of 5-HT on proteins D₁ to D₄. (A) Pleural sensory clusters from *Aplysia californica* were dissected and labeled with [³⁵S]methionine for 18 hours as described (8), and the ³⁵S-labeled proteins that react with MAB's 4E8 and 3D9 were immunoaffinity-purified (10). The labeled, immunoaffinity-purified proteins were mixed with unlabeled pleural sensory cluster proteins and resolved on a high resolution two-dimensional polyacrylamide gel (8). The gel was silver-stained to visualize total protein (left) and the ³⁵S-labeled proteins were visualized by autoradiography (right). (B and C) Pleural sensory clusters were dissected and labeled with [³⁵S]methionine under various experimental conditions. The proteins were then resolved on high-resolution two-dimensional gels (8); only the region of the gel containing proteins D₁ to D₄ is shown. (B) Serotonin (5 μM) for 30 minutes; 5-HT (5 μM) plus actinomycin D (100 μg/ml) for 30 minutes. This concentration of actinomycin D blocks more than 95 percent of RNA synthesis in *Aplysia* sensory neurons (5). (C) CFT-cAMP (100 μM) for 2 hours; 20 μM 5-HT plus 100 μM IBMX for 60 minutes.



M. Mayford, A. Barzilai, F. Keller, and E. R. Kandel are at the Howard Hughes Medical Institute and the Center for Neurobiology and Behavior, College of Physicians and Surgeons of Columbia University, 722 West 168 Street, New York, NY 10032. S. Schacher is at the Center for Neurobiology and Behavior, College of Physicians and Surgeons of Columbia University, 722 West 168 Street, New York, NY 10032.

*Present Address: Institut für Hirnforschung der Universität Zürich, August Forelstrasse 1, CH-8029 Zürich, Switzerland.

A

```

MDFAYIIIFVALLVLPICAGQEDDVTPEFVMIRPPLLEEDYLDLGESKTYTCGASATSDQVT 60
LKWFINDEQIETATSGRVRVEALGNSRYMLRIGSGEDNDGGVYRCETLAGQTDSTKINNV 120
VIKPLEIHSQEQFDILGGEVECEVSGKPAPTIVKFNENTKIEAGEKYTIALNKLII 180
KDLSEDTKKYLCDIIVIDTGETKDFYIDFTVVKLPTIALPPTIHPDNPKVGDEVKITCQ 240
ATGVPPPTYQFKGDMVMTDEMNNGLTINPLKTTDQATYTCIATNKGFAESSNTLDV 300
KVPPTIEDMEETDAVSGQELTITCTAKGDPSPVIVKDKGQPSASTGIVNKGPTYEKV 360
GSNQNDMEETKVAQHMTFKPVYQDAGTYICTAFSLVGSANKTVKLTQVKPKNFDTDFKE 420
REFFGWRGHKANLTCQANANPVATIEWYMPDAENDDYSKAVRIPNEAPYTNMLQKWDG 480
SFLSSRLSHVDIGDETSHYKDFCEATNVQGMIVQVVTLEAKPPGSPVISMGNVLTSSI 540
TVNIEPPAENNGQPVTEYTYLYYDPGDAATNNGQTARTGDKTLELTGLTNTFPYVVKV 600
KAKNNVGEGEATVTIPTLKVSKPFLRTIKSPQMSSENADSYLLEWEQPDGGSPIKHFSI 660
SYRQVKVKGTDPEGTWKIDGIDLDLPKLKVPNPNSALSTRLLDLDANAFYEIRLWATNEE 720

VGPVGDHSGRLAVNLAAALAPLACILAL* END d12:765
GDSLTQVLIKTSAGAEKEEKEEKEEKEEKEEKEEKEEKEEKEEKEEKEEKEEKEEKEEKEE 780

IGPVGDHSGRLAVNLAAALAPLACILAL* END d15:812
AGSSSAGLGGGVIIGIIVTLIVILLIVLLIIVFVTKKKPELVDRRLGRLGGKGGEEERGA 840
KDDGKDPAAEEELIKEDSVKVENEEENKPDQVIEEQPEEFEPETKPEPAEPATGPAPAE 900

ADAKPEDLPAPAPTEIKITPETPEKPNPPA* END d19:932

```

Gly, H, His; I, Ile; K, Lys; L, Leu; M, Met; N, Asn; P, Pro; Q, Gln; R, Arg; S, Ser; T, Thr; V, Val; W, Trp; and Y, Tyr. (B) A schematic representation of the domain organization of the three apCAM clones. Ig, immunoglobulin type c2 domain; Fn, fibronectin type III domain; GPI, glycosylphosphoinositol attachment signal; TM, transmembrane domain; CYTO, cytoplasmic domain; PEST, PEST sequence (22).

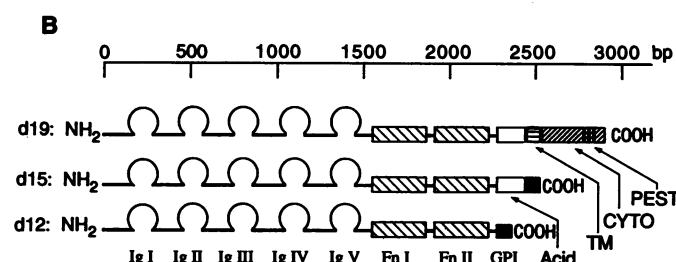


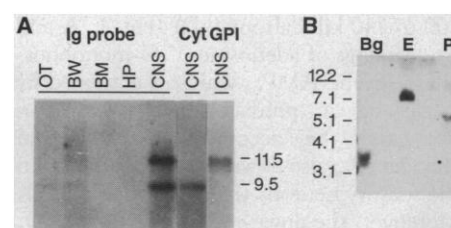
Fig. 2. Deduced amino acid sequence of apCAM. (A) An oligo(dT)-primed cDNA library was constructed in the expression vector λ gt11 Eco RI–Not I (Promega) with mRNA isolated from the CNS of *Aplysia californica* (31). The library was screened for plaques that cross-reacted with MAb's 4E8 and 3D9 (10). From approximately 500,000 recombinants, a single immunoreactive plaque was isolated that cross-reacted with both MAb 4E8 and 3D9. The cDNA insert from this clone was used to probe a randomly primed *Aplysia* CNS cDNA library constructed in the plasmid vector pBluescript II SK⁺ (Stratagene). The three resulting clones were sequenced on both strands with the standard dideoxy technique (Sequenase, USB). The three cDNA sequences were invariant over the 2252 nucleotides at the 5' end except for two positions that did not change the coded amino acid (GenBank accession numbers M89648 through M89650). Short stretches of hydrophobic amino acids that encode the signal peptide, the transmembrane domain, and a GPI attachment signal are underlined. The conserved cysteine residues in the five Ig domains are indicated with arrows. Two peptide sequences obtained from protein D₁ and from protein purified with MAb 4E8 are boxed. Abbreviations for the amino acid residues are as follows: A, Ala; C, Cys; D, Asp; E, Glu; F, Phe; G, Gly; H, His; I, Ile; K, Lys; L, Leu; M, Met; N, Asn; P, Pro; Q, Gln; R, Arg; S, Ser; T, Thr; V, Val; W, Trp; and Y, Tyr. (B) A schematic representation of the domain organization of the three apCAM clones. Ig, immunoglobulin type c2 domain; Fn, fibronectin type III domain; GPI, glycosylphosphoinositol attachment signal; TM, transmembrane domain; CYTO, cytoplasmic domain; PEST, PEST sequence (22).

lowed in each of the three clones by five immunoglobulin (Ig) domains of the C-2 type. These domains are characterized by conserved cysteine residues separated by 40 to 60 amino acids (12). The Ig domains are followed by two fibronectin type III domains (FnIII) (13). Because the overall structure is similar to that of Ig-related cell adhesion molecules, we have designated these molecules collectively as apCAM's, for *Aplysia* cell adhesion molecules.

The three apCAM clones diverge in sequence after the second FnIII domain. Clone d19 contains the longest open reading frame and encodes a protein with an acidic region consisting of a short stretch of amino acids rich in glutamate immediately after the second FnIII domain. This is followed by a stretch of 22 hydrophobic amino acids characteristic of a transmembrane domain, and a 117-amino acid putative cytoplasmic domain at the carboxyl terminus.

The clones with the two shorter open reading frames (d12 and d15) lack transmembrane and cytoplasmic domains. The d15 open reading frame contains, and d12 lacks, the glutamate-rich region. Both predicted proteins terminate in a short stretch of hydrophobic amino acids characteristic of proteins attached to the membrane via a glycosylphosphoinositol (GPI) linkage (14). Consistent with this observation,

Fig. 3. Structure of the apCAM gene. (A) Northern blot analysis of total *Aplysia* RNA (15 μ g) isolated from central nervous system (CNS), hepatopancreas (HP), buccal muscle (BM), body wall (BW), and ovotestis (OT). The RNA was isolated by the guanidinium isothiocyanate method and resolved on agarose formaldehyde gels. Blots were probed with ³²P-labeled cDNA fragments from the Ig region (nucleotides 1 to 1311) of apCAM. Filters were reprobated with cDNA fragments corresponding to the cytoplasmic domain of clone d19 (2536 to 2900) (Cyt) or the putative GPI signal region (2291 to 2426 of clone d12) (GPI). All filters were washed at high stringency [0.2 \times SSC, 0.1 percent SDS, 65°C] before exposure to x-ray film. (B) Southern blot analysis. *Aplysia* chromosomal DNA (10 μ g) was digested with Bgl II (Bg), Eco RI (E), or Pvu II (P) and resolved on agarose gels. Blots were probed with a ³²P-labeled cDNA probe from the third Ig domain (704 to 915), which is common to all three clones. Filters were washed as in (A).



bacterial phosphatidyl inositol-specific phospholipase C, which specifically cleaves GPI-linked proteins, released the 100-kD form of apCAM from CNS membranes (15). When deglycosylated, this form of apCAM can be resolved into two bands on SDS-polyacrylamide gels (16). This result suggests that D₁ actually contains two protein species and that the released material represents GPI-linked proteins encoded by transcripts specific for clones d12 and d15.

A Northern blot analysis of *Aplysia* RNA revealed two bands of 9.5 and 11.5 kilobases (kb), which were specific for nervous tissue (Fig. 3A). Rehybridization of the Northern blot with probes specific for the cytoplasmic domain of clone d19 and

for the GPI region of d12 and d15 indicated that the 9.5-kb mRNA contains the cytoplasmic domain sequences and the 11.5-kb band contains the two GPI forms. The finding of two rather than three bands presumably reflects the fact that clones d12 and d15 differ by only 144 nucleotides, and therefore their respective mRNA's would not be separable on the gels in Fig. 3A, and the 11.5-kb band is likely to contain both species. Moreover, the finding that the longer transcripts encode the smaller GPI-linked proteins may reflect the presence of additional untranslated sequences in these transcripts.

It is unclear how these three transcripts give rise to the four protein spots detected

on two-dimensional gels. D₁ may represent two protein species, while the remaining three apCAM species (116 to 140 kD) may arise from differences in posttranslational modification of the protein encoded by clone d19. Alternatively, they may arise from transcripts for which we have not yet obtained cDNA clones and that are not resolved on Northern blots.

The sequence and overall structural ar-

rangement of the three apCAM cDNA clones suggest that the different transcripts arise by alternative splicing of a single gene. To test this possibility, we probed a Southern blot of *Aplysia* chromosomal DNA with a 204-bp Hha I fragment (nucleotides 704 to 915), which is within the third Ig domain and therefore identical in all three clones. We detected a single major band in blots screened at high stringency (Fig. 3B).

Consistent with alternative splicing of a single gene, the 5' untranslated regions of the three clones are identical, and clones d15 and d12 share stretches of identical sequence in their 3' untranslated regions. These results are consistent with a single gene coding for the multiple apCAM transcripts.

The apCAM gene appears to be transcribed only in the CNS in the adult (Fig.

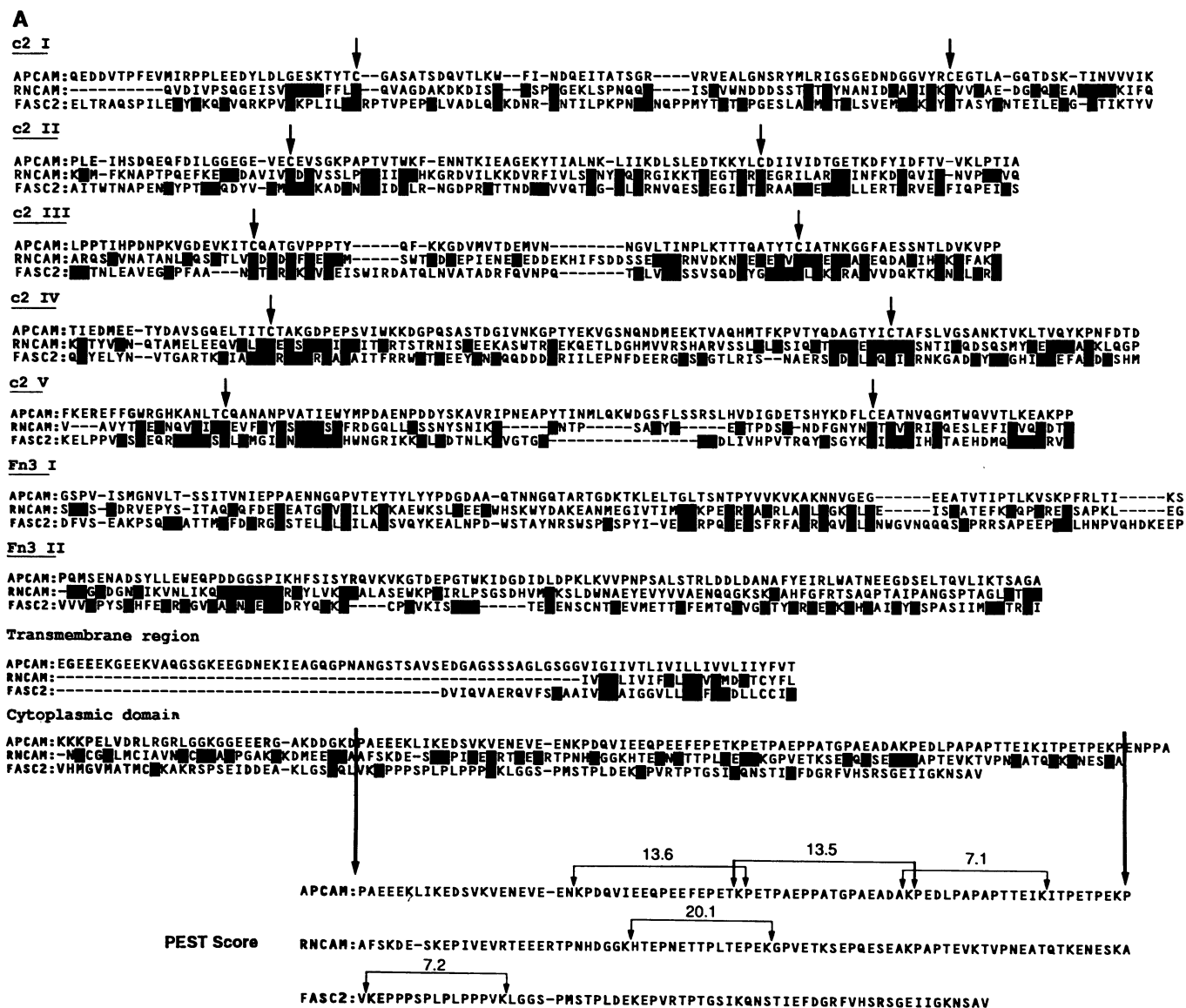


Fig. 4. Comparison of apCAM, rat NCAM, and *Drosophila* fasciclin II (FascII). (A) The amino acid sequence of apCAM was aligned to rat NCAM and *Drosophila* fasciclin II with the align function of DNA STAR (UW GCG). The apCAM clone d19 showed a 26 percent amino acid identity with rat NCAM and 24 percent identity with fasciclin II. The alignment was modified slightly by hand, and the cytoplasmic domains were aligned separately from the extracellular portion of the molecules. Amino acid identities are indicated by blackened squares. The conserved cysteine residue in the five Ig domains are indicated with arrows. The PEST sequences (bottom) in the cytoplasmic domain are indicated with scores calculated with the PEST-find algorithm (22). (B) Schematic representation of neural Ig molecules. The arrangement of Ig and F11 domains of neural Ig molecules (19) and apCAM.

3A), consistent with the distribution of apCAM protein (10). This restricted distribution in the adult differs from the general distribution during embryogenesis, where apCAM or apCAM-like protein is detected throughout the blastula stages of development (17). With the emergence of the

nervous system, apCAM disappears from all cells except neurons. In the nervous system, apCAM is expressed only on neurons and not on glial cells (10), and in particular on both the sensory and motor neurons of the gill-withdrawal reflex (see below). In the sensory neurons it is present in neurite

processes and is enriched at synaptic varicosities (10, 18).

The arrangement of Ig and FnIII domains in the apCAM's is similar to that of other glycoproteins expressed on the surface of developing axons, such as NCAM, L1, and TAG-1 in vertebrates and fasciclin II

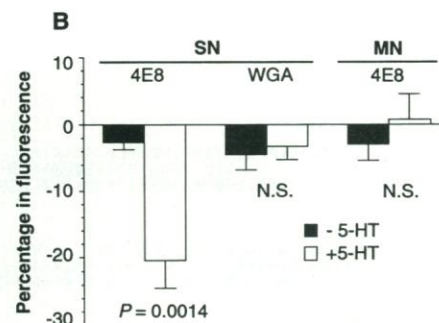
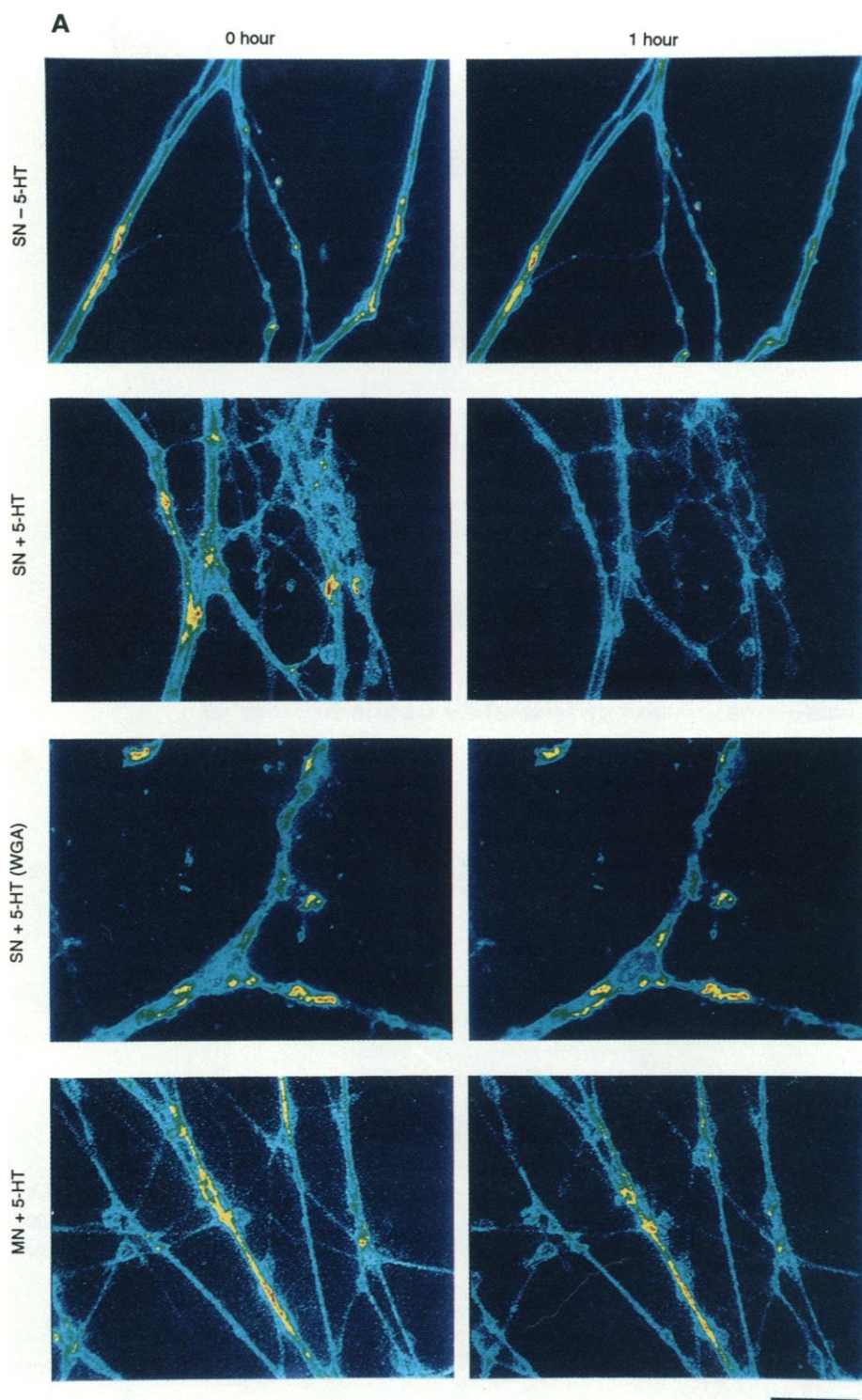


Fig. 5. Cell culture and fluorescent immunocytochemistry. **(A)** Mechanosensory cells from the pleural ganglion of adult animals and motor cell L7 from juvenile animals were plated and maintained in culture for 5 days as described (3, 4). Each culture dish contained either a single L7 motor cell or four to six sensory cells. Neurons were stained for 20 minutes with FITC-labeled MAb 4E8, for 45 minutes with FITC-labeled Fab' fragments of 4E8, or for 75 minutes with FITC-labeled WGA. Staining procedures were as described (10). Cultures were examined for epifluorescent staining with a Nikon Diaphot microscope and a Dage 66 SIT camera connected to a Dell computer with PC vision Plus frame grabber. All images were stored on a Storage Dimension Optical Disc for analyses. Immediately after the cells were viewed, each culture was treated with either control solution (L15 plus artificial seawater) or 2.5 μ M 5-HT in control solution for 1 hour. Cultures were rinsed and the same view areas were reexamined by using computer-aided superimposition of the live Nomarski optics image of the area with the previous image of the same area. Intensity of the fluorescent excitation of the cells, gain, and black levels were kept at the same manual setting for recording both images. Low levels of illumination were used to prevent photobleaching (pixel intensity range was 10 to 90 for both experimental and control; maximum in arbitrary units is 255). The intensity of staining is shown in pseudocolor (red is highest intensity and blue is lowest). **(B)** Summary of 5-HT effects on cell surface proteins. Four to six areas of neuritic outgrowth were examined on each motor cell (MN) and in each sensory cell (SN) culture for two to three cells selected at random. Each culture provided a single value for the change in the intensity of staining. The change in the intensity of the staining was obtained by averaging the peak intensity of staining before and after experimental treatment in six 25- μ m² regions selected at random from each view area. Thus, for each culture, 24 to 36 unit areas were compared

before and after treatment. For each view area, the image used for analysis was obtained by subtracting the background (to correct for slight changes in illumination from one time period to the next) and then was automatically computer enhanced. The high value was normalized to that obtained before treatment. N.S., not significantly different.

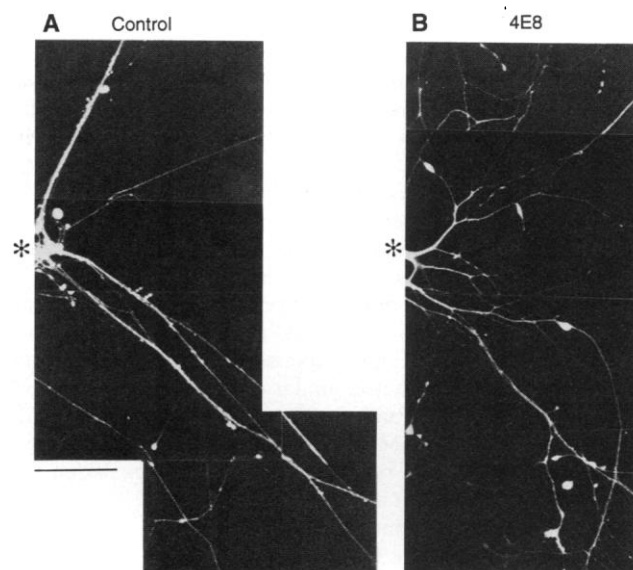
and neuroglian in invertebrates (19). These molecules mediate cell-cell adhesion as well as axon growth and guidance (20, 21). The observation that MAB's to apCAM cause defasciculated growth of cultured *Aplysia* neurons (10) is consistent with the protein functioning as a cell adhesion molecule.

When compared to the sequences of Ig-related cell adhesion molecules, apCAM shows the greatest overall similarity to NCAM and fasciclin II. Although the overall amino acid identity between optimally aligned sequences is only 26 percent and 24 percent, respectively, the general arrangement of the five Ig domains and the two FnIII domains is the same in all three molecules (Fig. 4). Also, all three molecules have forms that are GPI-anchored as well as forms that contain a transmembrane domain with conserved PEST sequences in the cytoplasmic region of the transmembrane form (Fig. 4). The PEST sequence is found in proteins with high turnover rates and is postulated to be involved in protein degradation (22). A conserved PEST sequence is also found in the cytoplasmic domain of the developmentally regulated cell surface molecules Notch and Xotch (23). Although it is not possible to assign unequivocally the functional homolog of apCAM among the Ig class of cell adhesion molecules, it is likely that apCAM, NCAM, and fasciclin II derive from a common ancestral gene.

Functional studies of apCAM. The 5-HT-induced down-regulation of apCAM (8) (Fig. 1) is achieved by a decrease in the amount of newly synthesized protein. To function in synaptic restructuring and growth, apCAM would need to be altered on the surface of neurites. To examine regulation of preexisting apCAM protein, we incubated fluorescein isothiocyanate (FITC)-labeled MAb 4E8 with cultured sensory neurons and measured the amount of fluorescence before and 1 hour after onset of 5-HT treatment (Fig. 5). In cultured sensory neurons, 5-HT produced a decrease of 20 ± 4 percent ($n = 7$) in the peak surface fluorescence compared to control cultures, which showed a decrease of 3 ± 3 percent ($n = 7$; $P < 0.002$; two-tailed t test). A similar decrease in immunofluorescence was seen when we used monovalent Fab' fragments of MAb 4E8 ($16 \pm 1\%$; $n = 4$; $P < 0.005$, two-tailed t test). We also tested the postsynaptic gill and siphon motor neuron L7 for apCAM regulation. Although the motor neuron responds in vivo to 5-HT, there was no change in the amount of surface apCAM immunofluorescence within 1 hour of exposure to 5-HT. Thus, the redistribution of surface apCAM induced by 5-HT is specific to the presynaptic sensory neuron.

To assess the molecular specificity of this

Fig. 6. Defasciculation of regenerating neurites of sensory cells by MAb 4E8 to apCAM. Fluorescent micrographs of neurites regenerated from the axon stump (*) from 3-day-old sensory cells after intracellular injection of 5(6)-carboxyfluorescein (4). Cells were treated with antibodies for 24 hours prior to injection. (A) IgG control. (B) MAb 4E8 (10). To quantitate differences in the pattern of growth, we counted the number of neurites intersecting a circle with a radius of $250 \mu\text{m}$ from the axon stump. Bar, $125 \mu\text{m}$.



response, we repeated the experiment on sensory neurons using FITC-conjugated wheat germ agglutinin (WGA) to stain neurite glycoproteins generally. We found no significant change in the amount of WGA-FITC bound to neurites 1 hour after 5-HT treatment (Fig. 5). This result suggests that 5-HT produces a selective effect on the distribution of apCAM protein in sensory neurons. However, Bailey and co-workers use a higher resolution method and can detect a slight decrease in surface WGA after treatment with 5-HT (18). Thus, it is likely that some surface proteins other than apCAM are also internalized in response to 5-HT.

The 5-HT-induced decrease in fluorescent labeling of sensory neurons could result from a redistribution of the protein, from release of the FITC-tagged MAb from the cell membrane, or from an internalization of the apCAM-MAB complex similar to that of receptor-mediated endocytosis (24). To distinguish among these possibilities, Bailey and co-workers (18) explored the alternative mechanisms of apCAM down-regulation with electron microscopy.

To examine the functional role of the down-regulation of apCAM on the growth of sensory neurons, we determined the effect of antibody to apCAM on sensory neurons in culture. In the absence of antibody, isolated *Aplysia* sensory neurons in culture grow out thick processes consisting of fascicles: bundles of fibers containing five to ten fine-diameter axons (4). In the presence of MAb 4E8, the bundles defasciculate, and the individual processes grow out alone (Fig. 6) (10). Treatment of control cultures of sensory neurons for 24 hours with MAb 4E8 caused a doubling in the number of neurite branch points in the treated cultures over that in control cultures (7.3 ± 1.4 branches in control and

15.1 ± 2.2 branches in treated cultures; $n = 10$, $P < 0.01$, two-tailed t test). The increase in branch points could result either from defasciculated growth or an actual stimulation of new neurite outgrowth in the presence of the antibody. This result is consistent with apCAM functioning in neuronal growth and remodeling.

Regulation of learning-related growth by cell adhesion molecules. During development, cell adhesion molecules mediate mechanical interactions between cells and contribute to axon growth and guidance in the nervous system (20, 21). For these purposes cell adhesion molecules are regulated over a time course of hours to days. Our data indicate that a cell adhesion molecule can also be modulated in the adult animal and that this modulation is triggered by neurotransmitters that mediate synaptic plasticity and synaptic reorganization. This modulation occurs in at least two ways: (i) down-regulation of the preexisting cell adhesion molecules on the surface of neurites and (ii) a decrease in the amount of newly synthesized apCAM protein in the cell body. The apCAM modulation is rapid, occurring within 1 hour after the addition of 5-HT. Finally, the down-regulation of newly synthesized protein appears to be mediated by cyclic AMP.

Functional studies of NCAM, the molecule to which apCAM shows the greatest similarity, indicated that the rate of adhesion of membrane surfaces varies as a third- or fourth-order function of the NCAM concentration (25). Thus, a twofold increase in the amount of NCAM on the cell surface produces a 30-fold increase in the rate of adhesion. Indeed, small changes in the amounts of NCAM can have significant effects on neurite outgrowth. When rat cerebellar neurons are plated on monolayers of cells expressing varying amounts of

NCAM, the extent of neurite outgrowth depends on the amount of substrate NCAM. Above a certain threshold, a 30 to 40 percent increase in substrate NCAM results in a twofold increase in neurite outgrowth (26).

In *Aplysia*, 5-HT produces a decrease in the amount of apCAM on the surface of the sensory neuron without producing a concomitant decrease in apCAM on its substrate, the postsynaptic motor neuron. As a result, 5-HT leads to a change in the relative amount of apCAM expression on neurite and substrate that is similar to that seen in the vertebrate studies with NCAM. If the amount of apCAM on the surface of the sensory and motor neurons is close to the threshold needed for adhesion, then the shift in the relative amounts of apCAM might contribute to the outgrowth of sensory neurites on the motor neurons and the formation of new synaptic structures by these neurons. A parallel is found in the developing vertebrate neuromuscular junction, where a presynaptic decrease in NCAM function, through the addition of polysialic acid, leads to enhanced neurite outgrowth onto the postsynaptic target (27).

How cell adhesion molecules influence neurite growth is unclear. Although there appears to be no simple relation between the amount of cell adhesion and growth (28), the loss of a cell adhesion molecule may lead to unrestricted growth in colorectal cancers (29). Moreover, in the developing nervous system, the down-regulation of NCAM precedes the migration of neural crest cells (30). Thus, the reduction of apCAM in the sensory neurons may relieve an inhibition on growth, specifically on the

movement of neurites of the sensory neurons on their motor neuron substrate.

In *Aplysia*, exposure of stable sensory-motor cocultures to 5-HT, a procedure that decreases within 1 hour the expression of the NCAM-like cell adhesion molecule apCAM in the presynaptic neurons, results in an increased number of synaptic varicosities 24 hours later (7). Bailey and co-workers (18) examined the mechanism of the surface apCAM modulation and found a 50 percent loss of apCAM protein from the cell surface via endocytosis. The isoforms of apCAM that are down-regulated at the cell surface and the identity of the second messenger systems mediating this regulation remain to be determined.

REFERENCES AND NOTES

1. C. H. Bailey and M. Chen, *Proc. Natl. Acad. Sci. U.S.A.* **85**, 2372 (1988); *ibid.*, p. 9356; *J. Neurosci.* **9**, 1774 (1989).
2. E. Fiková and A. Van Harreveld, *J. Neurocytol.* **6**, 211 (1977); K. S. Lee, F. Schottler, M. Oliver, G. Lynch, *J. Neurophysiol.* **44**, 247 (1980); F.-L. Change and W. T. Greenough, *Brain Res.* **309**, 35 (1984); N. L. Desmond and W. B. Levy, *ibid.*, p. 476.
3. S. G. Rayport and S. Schacher, *J. Neurosci.* **6**, 759 (1986).
4. D. L. Glanzman, E. R. Kandel, S. Schacher, *Neuron* **3**, 441 (1989).
5. P. G. Montarolo *et al.*, *Science* **234**, 1249 (1986).
6. D. L. Glanzman *et al.*, *J. Neurosci.* **9**, 4200 (1989).
7. D. L. Glanzman, E. R. Kandel, S. Schacher, *Science* **249**, 799 (1990).
8. A. Barzilai, T. E. Kennedy, J. D. Sweatt, E. R. Kandel, *Neuron* **2**, 1577 (1989).
9. S. Schacher, V. F. Castellucci, E. R. Kandel, *Science* **240**, 1667 (1988); P. G. Montarolo, D. L. Glanzman, E. R. Kandel, S. Schacher, *Soc. Neurosci. Abstr.* **17**, 1591 (1991).
10. F. Keller and S. Schacher, *J. Cell Biol.* **111**, 2637 (1990).
11. G. von Heijne, *Nucleic Acids Res.* **14**, 4683 (1986).
12. A. F. Williams and A. N. Barclay, *Annu. Rev. Immunol.* **6**, 381 (1988).
13. R. O. Hynes, *Annu. Rev. Cell Biol.* **1**, 67 (1986).
14. M. A. J. Ferguson and A. F. Williams, *Annu. Rev. Biochem.* **57**, 285 (1988).
15. M. Mayford and F. Keller, unpublished data.
16. F. Keller, unpublished data.
17. S. Schacher *et al.*, *Cold Spring Harbor Symp. Quant. Biol.* **55**, 187 (1990).
18. C. H. Bailey, M. Chen, F. Keller, E. R. Kandel, *Science* **256**, 645 (1992).
19. A. J. Furley *et al.*, *Cell* **61**, 175 (1990); A. L. Harrelson and C. S. Goodman, *Science* **242**, 700 (1988); M. Moos *et al.*, *Nature* **334**, 701 (1988); B. A. Cunningham *et al.*, *Science* **236**, 799 (1987); A. J. Bieber *et al.*, *Cell* **59**, 447 (1989).
20. G. M. Edelman, *Annu. Rev. Cell Biol.* **2**, 81 (1986); T. M. Jessell, *Neuron* **1**, 3 (1988).
21. G. Greeningloh, E. J. Rehm, C. S. Goodman, *Cell* **67**, 45 (1991).
22. M. Rechsteiner, *Adv. Enzyme Regul.* **27**, 135 (1988).
23. C. Coffman, W. Harris, C. Kintner, *Science* **249**, 1438 (1990).
24. W. B. Huffner *et al.*, *Curr. Opin. Neurobiol.* **1**, 388 (1991).
25. S. Hoffman and G. M. Edelman, *Proc. Natl. Acad. Sci. U.S.A.* **80**, 5762 (1983).
26. P. Doherty *et al.*, *Nature* **343**, 464 (1990); P. Doherty, L. H. Rowett, S. E. Moore, D. A. Mann, F. S. Walsh, *Neuron* **6**, 247 (1991).
27. L. Landmesser, L. Dahm, J. Tang, U. Rutishauser, *Neuron* **4**, 665 (1990).
28. V. Lemmon, S. M. Burden, H. R. Payne, G. J. Elmslie, M. L. Halvin, *J. Neurosci.* **12**, 818 (1992); U. Rutishauser, A. Acheson, A. K. Hall, D. M. Mann, J. Sunshine, *Science* **240**, 53 (1988); P. M. Doherty, J. Cohen, F. S. Walsh, *Neuron* **5**, 209 (1990).
29. E. R. Fearon *et al.*, *Science* **247**, 49 (1990); K. Vlemminckx, L. Vakaet, Jr., M. Mareel, W. Fiers, F. Van Roy, *Cell* **66**, 107 (1991).
30. J.-P. Thiery, J.-L. Duband, U. Rutishauser, G. M. Edelman, *Proc. Natl. Acad. Sci. U.S.A.* **79**, 6737 (1982).
31. J. Sambrook, E. F. Fritsch, T. Maniatis, *Molecular Cloning: A Laboratory Manual* (Cold Spring Harbor Laboratory, Cold Spring Harbor, NY, 1989).
32. We thank R. Axel, T. Jessell, and F. Maxfield for their comments on this manuscript and K. Raguvian, K. Hiltner, and S. Mack for technical assistance. Supported by the Howard Hughes Medical Institute, an NIH grant (S.S.), and Stiftung für medizinisch-biologische Stifendion (F.K.).

26 November 1991; accepted 1 April 1992